Light Stable Isotope (O, H, C) Signatures of BIF-Hosted Iron Ore Systems: Implications for Genetic Models and Exploration Targeting

Steffen Hagemann, Ana-Sophie Hensler, Rosaline Cristina Figueiredo e Silva, and Harilaos Tsikos

Abstract

Stable isotope data from hypogene (i.e., below the line of weathering) iron oxides and gangue minerals from BIF-hosted iron ore deposits in Australia, South Africa, and Brazil have significantly assisted in constraining different hydrothermal fluid sources and fluid flow models during the upgrade of BIF to iron ore. The $\delta^{18}O$ values on iron oxides from BIF and different paragenetic stages of enrichment display a consistent decrease from unenriched BIF (4–9‰) to as low as −10‰ for high-grade iron ore. This large shift in oxygen isotope values is interpreted as evidence for enormous incursion of 'ancient' meteoric water into fault and fracture zones at the time of iron enrichment during the Archean and Paleoproterozoic time. The $\delta^{18}O_{fluid}$ values of paragenetically early iron oxides of > 4‰ suggest the involvement of magmatic fluids in greenstone belt-hosted Carajás-type iron ore deposits, and basinal brines in basin-hosted Hamersley-type deposits. In contrast, the paragenetically late stage iron oxides in the metamorphosed, basin hosted iron ore deposits of the Quadrilátero Ferrífero display $\delta^{18}O_{fluid}$ values > 6‰. This reflects the renewed deep crustal, hypogene (metamorphic or magmatic) fluid influx. Carbon and oxygen isotope data on carbonates in BIF and hydrothermally altered iron ore indicate that carbon in the latter is not derived from BIF units, but represents either magmatic carbon in the case of the Carajás-type deposits or carbon within the underlying basin stratigraphy as in the case of the Hamersley-type iron deposits. The systematic decrease of $\delta^{18}O$ values in iron oxides from the early to late paragenetic stages and from the distal to proximal alteration zone, including the ore zone, may be used as a geochemical vector. In this case, oxygen isotope analyses on iron oxides provide a potential exploration tool, particularly for targeting the extension of iron ore bodies or entirely concealed high-grade iron ore deposits, in which hematite/magnetite are frequently the only mineral that can be readily analysed.

S. Hagemann (✉)
Centre for Exploration Targeting, School of Earth Sciences, University of Western Australia, Crawley, WA 6009, Australia
e-mail: Steffen.Hagemann@uwa.edu.au

A.-S. Hensler
Institute of Mineral Resources Engineering, RWTH Aachen University, 52062 Aachen, Germany

R. C. Figueiredo e Silva
Universidade Federal de Minas Gerais, Centro de Pesquisas Prof. Manoel Teixeira da Costa-Instituto de Geociências, Av. Antônio Carlos 6627, Campus Pampulha, Belo Horizonte, MG 31270.901, Brazil

H. Tsikos
Department of Geology, Rhodes University, Grahamstown 6140, South Africa

D. Huston and J. Gutzmer (eds.), *Isotopes in Economic Geology, Metallogenesis and Exploration*, Mineral Resource Reviews, https://doi.org/10.1007/978-3-031-27897-6_12

Keywords

BIF · Iron · Oxygen carbon isotopes · Genetic model · Targeting

1 Introduction

Stable isotope analyses are a relatively new approach in the Banded Iron Formation (BIF)-hosted iron ore system and have only been applied in the past three decades. Stable isotope analyses, however, can add fundamental information to our understanding of iron ore genesis, particularly because detailed deposit-scale investigations in Australia, Brazil and Africa have shown that hydrothermal fluids play a significant role in the upgrade of BIF to iron ore (e.g., Hagemann et al. 1999; Thorne et al. 2004; Cope et al. 2008, Rosière et al. 2008; Spier et al. 2008; Cabral and Rosiere 2013; Figueiredo e Silva et al. 2013; Hensler et al. 2015).

The purpose of this review is to summarize the impact of stable isotope geochemistry on the understanding of the BIF-hosted iron ore systems. In addition, potential applications of stable isotope analyses for the exploration of concealed iron deposits or extension of existing iron ore systems are discussed.

The first part of this review provides a summary of data for the major BIF-hosted iron systems in the world, namely the Hamersley (Australia), Transvaal and the Griqualand West (South Africa), Pic de Fon (West Africa), Quadrilátero Ferrífero (QF, Brazil), Carajás (Brazil), Urucum (Brazil), and Noamundi (India). The second part summarizes the genetic implications of the stable isotope data. The last part provides examples of how stable isotope data can be applied in exploration and discuss its limitations.

2 Review of Significant BIF-Hosted Iron Ore Districts and Deposits

The BIF-hosted iron ore system represents the world's largest and highest grade iron ore districts and deposits (Fig. 1). Banded iron-formation, the precursor to low- and high-grade BIF-hosted iron ore, consists of Archean and Paleoproterozoic Algoma-type BIF (e.g., Serra Norte iron ore district in the Carajás Mineral Province), Proterozoic Lake Superior-type BIF (e.g., deposits in the Hamersley province, and deposits in the Quadrilátero Ferrífero), and Neoproterozoic Rapitan-type BIF (e.g., the Urucum iron ore district). The following sections briefly review the major iron ore districts in the world; many of those are currently in production. Due to the different level of investigations, the information about different deposits and districts is inconsistent. All references to production or reserves below refer to Fe ore.

2.1 Precambrian BIF-Hosted Iron Ore Districts of Western Australia

The three major BIF-hosted iron ore provinces in Western Australia (Fig. 1; Hagemann et al. 2016, 2017) are the: (1) Hamersley province, which hosts the giant Mt Whaleback (1800 Mt), Mt Tom Price (900 Mt) and Paraburdoo (800 Mt) deposits, and the Mining Area C (950 Mt), and Chichester Range (2230 Mt) districts, (2) Yilgarn craton, which contains a large number of small to medium size (50–150 Mt) deposits such as Koolyanobbing (93 Mt; including Windarling), Wiluna West (78 Mt—not actively mined), Wiluna and Jack Hills (78 Mt—not actively mined), and (3) Pilbara craton with small to medium size iron ore districts in the central Pilbara, for example McPhee Creek (136 Mt), Mt Goldsworthy (122 Mt; including Nimingarra, Shay Gap, Sunrise Hill and Yarrie), Mt Webber (39 Mt) and Corunna Downs (37 Mt), and the western Pilbara that hosts lower-grade (when compared to the central part), primary magnetite-rich BIF, including Cape Lambert (485 Mt), Miaree (90 Mt), and Mt Oscar (43 Mt). Presently, only the Mt Webber deposit is in production.

The Hamersley province hosts two major BIF-hosted iron ore styles (Hagemann et al. 2017 and references therein): (1) high-grade (59–64 wt.-% Fe) hematite ore (commonly referred to as "blue" ore in the Hamersely Province of Western

Fig. 1 Location of significant BIF-hosted iron ore districts and deposits. The cumulative length of the bar graphs beneath each locality indicates the Fe grade

Australia), which, in many localities, is accompanied by minor martite-microplaty hematite ore, but contains little or no goethite ore, is mostly confined to the Brockman Iron Formation; and (2) high-grade (58–62 wt.-% Fe) martite-goethite ores ("brown" ore) of the Marra Mamba and Brockman Iron Formation.

In the Yilgarn craton, martite-goethite ores are located at all major deposits; specular hematite ore is best developed at the Koolyanobbing and Weld Range deposits (Duuring et al. 2017a). Magnetite-martite ores are common at Koolyanobbing, Weld Range and Matthew's Ridge, whereas microplaty hematite-martite-specular hematite ore is more common at Windarling and Wiluna West (Duuring et al. 2017a).

In the Pilbara craton most deposits display broad, near-surface, supergene goethite ± martite ores that constitute the bulk of the high-grade iron ore, although narrower hypogene magnetite ± hematite ore zones are recognised in deeper parts of most iron ore deposits (Duuring et al. 2017b).

According to Hagemann et al. (2017) BIF-hosted iron ore deposits in the Hamersley province, Yilgarn and Pilbara cratons are classified as: (1) granite-greenstone belt hosted, fault zone controlled with mineralising fluids derived from magmatic (± metamorphic) sources, together with ancient, warm meteoric waters (most of the deposits in the Yilgarn and Pilbara cratons, such as Koolyanobbing or Mt Webber, belong to this type); (2) sedimentary basin-hosted that are fault controlled, (mostly normal faults), and mineralising fluids sourced from early basinal (evaporitic) brines and ancient, warm meteoric waters. These deposits contain martite-microplaty hematite as their main ore minerals and are exemplified by the giant deposits located in the Hamersley province, such as Mt Tom Price or Mt Whaleback; and (3) martite-goethite iron ore deposits, such as Mining Area C in the Hamersley

province, which are supergene-enriched via interaction of BIF with Cretaceous to Paleocene cold meteoric waters (Morris and Kneeshaw 2011) that gained access to the deposit site via already emplaced ancient fault systems and as a result of the interplay between exhumation and surface modification. These deposits have no evidence for deep hypogene roots.

2.2 Precambrian BIF-Hosted Iron Ore Districts of Africa

2.2.1 Kapvaal Craton in South Africa

Commercial South African iron-ore deposits associated with BIF are located in the Transvaal and Griqualand West segments of the Neoarchaean to Palaeoproterozoic Transvaal Supergroup (Fig. 1). Since closure of the Thabazimbi Mine in 2015 (Anglo American Press Release, 16/07/2015), the Griqualand West area has become essentially the only productive region in terms of volume and spatial distribution of iron ore. Four deposits account for practically the entire annual production in South Africa, which at 2014 amounted to 78 Mt of high-grade ore (Smith and Beukes 2016). These deposits are Sishen and Kolomela (also previously known as Sishen South), operated by Kumba Iron Ore, and Khumani and Beeshoek, operated by Assmang Ltd. All deposits occur on a roughly N–S trend that connects the towns of Sishen and Postmasburg, the latter respectively situated at the northernmost and southernmost extremities of a doubly-plunging anticline locally known as the Maremane Dome. Several smaller deposits and occurrences of iron ore that have attracted attention in the broader Maremane area (Land 2013) include Demaneng, Kapstevel, Doornpan, Kareepan, MaCarthy, or Welgevonden.

The prevailing geological setting of the iron-ore deposits at the Maremane Dome involves karstification of Campbellrand dolostones at the stratigraphic base of the Transvaal Supergroup, followed by collapse of overlying Asbesheuwels BIF into karstic sinkholes and apparent replacement thereof by massive hematite. Texturally, the ores range from massive to laminated, breccia and conglomeratic types. On a regional scale, these karst-hosted iron ore deposits are located immediately below an angular unconformity, where the Asbesheuwels BIF (mainly the Kuruman Member) is directly overlain by red-beds of the late Paleoproterozoic Olifantshoek Supergroup (Gamagara-Mapedi formations: Beukes et al. 2003; Smith and Beukes 2016). An ancient supergene model is, therefore interpreted to be the central ore-forming mechanism, under conditions of lateritic weathering involving intense leaching of silica and largely residual iron enrichment as ferric oxides at the expense of BIF (Smith and Beukes 2016).

Apart from the supergene class, smaller and generally sub- to uneconomic iron ore deposits of a hydrothermal origin are also present in the Transvaal and Griqualand West areas, with the Thabazimbi deposit being, until recently, the economically most significant from the Transvaal area (Netshiowi 2002). Hypogene iron ore at Thabazimbi is interpreted to have formed by hydrothermal replacement of Penge BIF, temporally linked to folding and thrusting (Basson and Koegelenberg 2017). The Penge BIF is the stratigraphic equivalent to the Kuruman BIF from the Griqualand West Basin. Minor deposits of similar hydrothermal affinity are also known from Giqualand West in association with the Rooinekke BIF of the Koegas Subgroup (Smith and Beukes 2016).

2.2.2 West African Craton in Guinea

BIF-hosted iron ore deposits of West Africa are epitomised by the Pic de Fon deposit (Cope et al. 2008). The deposit has a strike length of 7.5 km and width of approximately 0.5 km, and is located at the southern end of the Simandou Range in SE Guinea. The ore-bearing stratigraphy consists of three BIF intervals of which the top two have undergone selective enrichment into massive iron oxide ore (up to 65 wt.-% Fe) over thicknesses as much as 250 m. Predominant iron oxide phases are, in paragenetic order, recrystallised martite (after magnetite), hematite overgrowths and bladed microplaty hematite replacing gangue. Chemical mass balance calculations suggest that iron ore formation at Pic de

Fon involved primarily conservative iron enrichment through silica leaching, although net addition of iron up to 36% is also locally observed. Fluid circulation at Pic de Fon was likely driven by post-Eburnean (2.1–2.0 Ga) orogenic collapse or later Proterozoic thermal events, with possible generation of late-stage microplaty hematite during the Pan-African orogeny at 750–550 Ma (Cope et al. 2008).

2.3 Precambrian BIF-Hosted Iron Ore Districts of Brazil

Brazil contains three major BIF-hosted iron ore districts: the Quadrilátero Ferrífero (QF) iron ore province, Carajás Mineral Province (CMP), and Urucum district. The following sections will provide a brief geological overview.

2.3.1 Quadrilátero Ferrífero Province

The QF iron ore province (Fig. 1) is the largest known accumulation of single itabirite-hosted iron ore bodies worldwide with ore reserves of about 9 Gt (52 wt-% Fe, Ministério de Minas e Energia 2009) and over 3.5 Gt of high-grade iron ore (> 65 wt-% Fe; Rosiere et al. 2008). Major ore deposits that are currently under exploitation are e.g. Casa de Pedra (>1.2 Gt high-grade ore), Capitão do Mato (>147 Mt high-grade ore) and Conceição (>470 Mt high-grade ore: Rosière et al. 2008). Most of the iron ore bodies of the QF consist of massive and schistose hypogene iron ore with subordinate supergene iron ore present in the weathering horizons. The hypogene-supergene iron ore is characterized by a complex iron (hydr-) oxide paragenetic sequence including: (itabirite-hosted) magnetite → (itabirite-hosted) martite → (massive ore-hosted) martite → (massive ore-hosted) granoblastic hematite → (massive and schistose-ore hosted) microplaty hematite → (schistose ore- and shear zone-hosted) specular hematite → (lateritic ore-hosted) goethite (e.g., Rosière et al. 2008; Spier et al. 2008; Cabral and Rosière 2013; Hensler et al. 2015). The different iron oxide generations are the result of either replacement (e.g. for martite, granoblastic hematite) or precipitation (e.g. specular hematite) processes (Rosière et al. 2008; Hensler et al. 2015; Oliveira et al. 2015).

Laser ablation-ICP-MS mineral chemical analysis of hypogene iron oxides from QF itabirite and related ore revealed trace element and REE chemical signatures that are distinct for the specific iron oxide generations (Hensler et al. 2015). Major mineralogical and chemical trends include: (i) martitisation, which is accompanied by an absolute depletion of Mg, Mn, Al, Ti and enrichment of Pb, As and light rare earth elements (LREE) in martite; (ii) recrystallisation of magnetite (and martite) to granoblastic and locally microplaty hematite is an "isochemical" process, in which major chemical changes are absent; and (iii) schistose specular hematite is trace element- and REE-depleted. The mineral chemical changes from one iron oxide generation to another one are interpreted to reflect distinct mineralisation events, changing fluid conditions and different fluid/rock ratios.

2.3.2 Carajás

The Carajás iron ore deposits are located in the eastern part of the state of Pará with reserves of 17 Gt (>64 wt.-% Fe). The deposits are hosted by an Archean metavolcano-sedimentary sequence, and protoliths to iron mineralization are jaspilites, under- and overlain by basalts, both of which are greenschist-facies metamorphosed. The major Serra Norte N1, N4E, N4W, N5E and N5S iron ore deposits in the CMP are distributed along, and structurally controlled by, the northern flank of the Carajás fold (Rosière et al. 2006). Varying degrees of hydrothermal alteration have affected jaspilites to form high-grade iron ores (Figueiredo e Silva et al. 2008, 2013; Lobato et al. 2008) from distal to proximal zones. The least-altered jaspilite contains portions of hematite-free, recrystallised chert in equilibrium with magnetite, interpreted as the early stage of hydrothermal alteration. Variably altered jaspilites may be brecciated, containing various amounts of hematite types (e.g. microplaty and anhedral), and vein-associated quartz, carbonate and sulphide minerals. A hydrothermal paragenetic sequence for the oxides is established from

the earliest magnetite → martite → microplaty hematite → anhedral hematite (AnHem)- to the latest → euhedral-tabular hematite (EHem-Them).

Other mineralogical modifications are: (i) recrystallisation and cleansing of jasper with formation of chert and fine quartz; (ii) progressive leaching of chert and quartz, leaving oxides and a significant volume of empty space; (iii) silicification and dolomitisation with associated sulphides and oxides in veins, breccias and along jaspilite bands; (iv) advanced martitisation with the formation of AnHem, partial microcrystalline hematite recrystallisation to AnHem and partial open-space filling with microplaty/platy hematite; and (v) continued space-filling by comb-textured EHem and THem in veinlets and along bands.

2.3.3 Urucum

The Urucum manganese and iron ore mining district is located in the Mato Grosso state near the Brazilian-Bolivian border and consists of several open pit mines (e.g. Mineração Corumbaense Reunida, Urucum Mineração mine). In 2005, reserves were estimated at about 3.1 Gt of iron ore and 11 Mt of manganese ore (DNPM 2005; Walde and Hagemann 2007).

The iron ore is hosted in the Neoproterozoic metasedimentary rocks of the Santa Cruz Formation of the Jacadigo Group, which contains mainly hematite-rich BIFs and Mn ore horizons with subordinate interbedded arkosic sandstone (Urban et al. 1992; Walde and Hagemann 2007; Piacentini et al. 2013). The protore BIFs are interpreted to have been deposited in a glaciomarine environment (e.g. Urban et al. 1992; Klein 2005; Angerer et al. 2016). Recent petrographic-mineralogical studies of the Santa Cruz ore deposit (Angerer et al. 2016) distinguish between a dolomite-chert-hematite BIF (35–52 wt.-% Fe) in an upper and lower carbonaceous zone and chert-hematite BIF (45–56 wt.-% Fe) of an intermediate siliceous zone. Deci- to meter-thick diamictic hematite-rich chert (~16 wt.-% Fe) and mud (59–66 wt.-% Fe) layers are discontinuously intercalated in the BIFs (Angerer et al. 2016). Iron oxides of the BIFs are mainly fine-grained (grain sizes < 20 µm) anhedral to microplaty hematite. Locally microplaty hematite is oriented parallel to the bedding. Beside gangue minerals, diamictic hematite-rich chert layers contain microcrystalline (grain sizes of 10–20 µm) hematite "needles" and are interpreted to represent a replacement product of fibrous silicates. In the hematite-rich mud layers, different hematite variations are present ranging from relict hematite to granoblastic hematite.

The exact genesis of the ore deposits of the Urucum mining district is still ambiguous (e.g. Dorr 1964; Trompette et al. 1998; Walde and Hagemann 2007; Viehmann et al. 2016). This is mainly because most studies (e.g. Graf et al. 1994; Trompette et al. 1998; Freitas et al. 2011; Piacentini et al. 2013; Angerer et al. 2016; Viehmann et al. 2016) concentrated on the depositional conditions of the protore BIFs during the Neoproterozoic times rather than on the post-depositional modification and upgrade of the BIF to iron ore. Walde and Hagemann (2007), however, favoured a genetic ore model that includes the input of hypogene hydrothermal activity during the upgrade of the protore BIF and iron ore formation of Urucum, because of some mineralogical features of the ore, such as (1) the presence of braunite as indicator for elevated temperatures; (2) the presence of magnetite along fault zones; and (3) the emplacement of quartz-tourmaline veins crosscutting the Jacadigo Group. Gutzmer et al. (2008) argue based on detailed whole rock and trace element geochemistry analyses of high-grade ore samples that supergene processes played a major role in the formation of the Urucum iron ore district. However, most recent geochemical investigations of the BIFs from the Urucum district (Angerer et al. 2016; Viehmann et al. 2016) could not observe any geochemical evidence for a significant overprint and post-depositional alteration of the Urucum successions.

2.4 India

The high-grade (>60 wt.-%) iron ore deposits (e.g. Noamundi, Kiriburu, Megthaburu, Joda) of the Noamundi area are located in the north eastern part of India and hosted in the iron formations of

the metasedimentary greenstone belt sequence of the Archean Western Iron Ore Group (Beukes et al. 2008; Roy and Venkatesh 2009; Bhattacharya and Ghosh 2012). The overall annual iron ore production of the entire mining area is about 12 Mt and resources are estimated to be about 3.3 Gt of high-grade iron ore (Bhattacharya and Ghosh 2012). The unaltered protore BIF is approximately 220 m thick and mainly consists of thin, alternating chert- and hematite-magnetite-rich mesobands. High-grade iron ore of the Noamundi mining area can be separated in upper goethite- and lower hematite-rich iron ore. Goethite-rich ore is mainly associated with reworked canga-type successions related to erosion of Cretaceous to early Cenozoic land surface. Hematite-rich ore accounts for the major part of the iron ore resources and can be subdivided into hard and soft-friable ore (Beukes et al. 2008; Bhattacharya and Ghosh 2012). The former is present particularly in the lower successions of the iron ore bodies, whereas the latter is located mainly in the saprolitic weathering zone of the ore body. The hematite-rich iron ore contains different generations of hematite (e.g. euhedral, anhedral, cryptoplaty and microplaty) with minor relict magnetite, martite and goethite.

Hard high-grade iron ore of the Noamundi mining area is interpreted to have formed by hydrothermal processes, involving the dissolution of quartz, likely cogenetic crystallisation of magnetite, subsequent martitisation and precipitation of microplaty hematite (Beukes et al. 2008; Roy and Venkatesh 2009; Bhattacharya and Ghosh 2012). Friable hematite-rich as well as goethite-rich ores are interpreted to have largely formed and/or been overprinted by supergene lateritic processes during Cretaceous-Cenozoic times (Beukes et al. 2008).

3 Oxygen, Hydrogen, Carbon Isotope Data of BIF and Related Iron Ore

Presently there are significant stable isotope data sets for BIF-hosted iron ore deposits and districts from Western Australia, South Africa, Guinea, Brazil and India (Fig. 1). The following sections review these data sets and their interpretation in the regional context. All $\delta^{18}O$ and δD values are presented in‰ relative to Vienna Standard Mean Ocean Water (VSMOW), whereas $\delta^{13}C$ and $\delta^{18}O$ on carbonates are shown in‰ relative to Vienna Pee Dee Belemnite (VPDB).

3.1 Western Australia

Stable isotope data sets, mainly oxygen on quartz and oxides, as well as carbon and oxygen on carbonates are available for the Hamersley province and the Yilgarn and Pilbara cratons (Fig. 2).

3.1.1 Oxygen Isotope Data on Iron Oxides and Silicates

Thorne et al. (2004) presented detailed oxygen isotope data sets on quartz and oxides from the Tom Price, Paraburdoo and Channar deposits. The $\delta^{18}O$ values of magnetite and hematite from hydrothermal alteration assemblages and high-grade iron ore range from −9.0 to −2.9‰, and thus are depleted up to 5–15‰ relative to the magnetite of the host BIF (Fig. 2).

Thorne et al. (2009) calculated the oxygen isotope composition of hydrothermal fluids ($\delta^{18}O_{fluid}$) in equilibrium with iron oxides using the isotope fractionation of Becker and Clayton (1976) for magnetite and of Yapp (1990) for hematite and temperatures based on the fluid inclusion trapping temperatures from BIF, hydrothermal alteration assemblages, and high-grade iron ores. Trapping temperatures were pressure-corrected using stratigraphic reconstructions of the Mt. Tom Price deposit (30 °C: Taylor et al. 2001; Thorne et al. 2004) and the Paraburdoo (40 °C) and Channar deposits (30 °C; Dalstra 2006) during the likely time of hydrothermal alteration in the Paleoproterozoic.

The range of $\delta^{18}O_{fluid}$ values for all of the Hamersley iron ore deposits is shown in Fig. 2. At Tom Price they range from 12.7 to 21.7‰ for magnetite of the Dales Gorge and Joffre BIF members, from −0.7 to −0.4‰ for magnetite in distal alteration zones, from −3.5 to 1.2‰ for

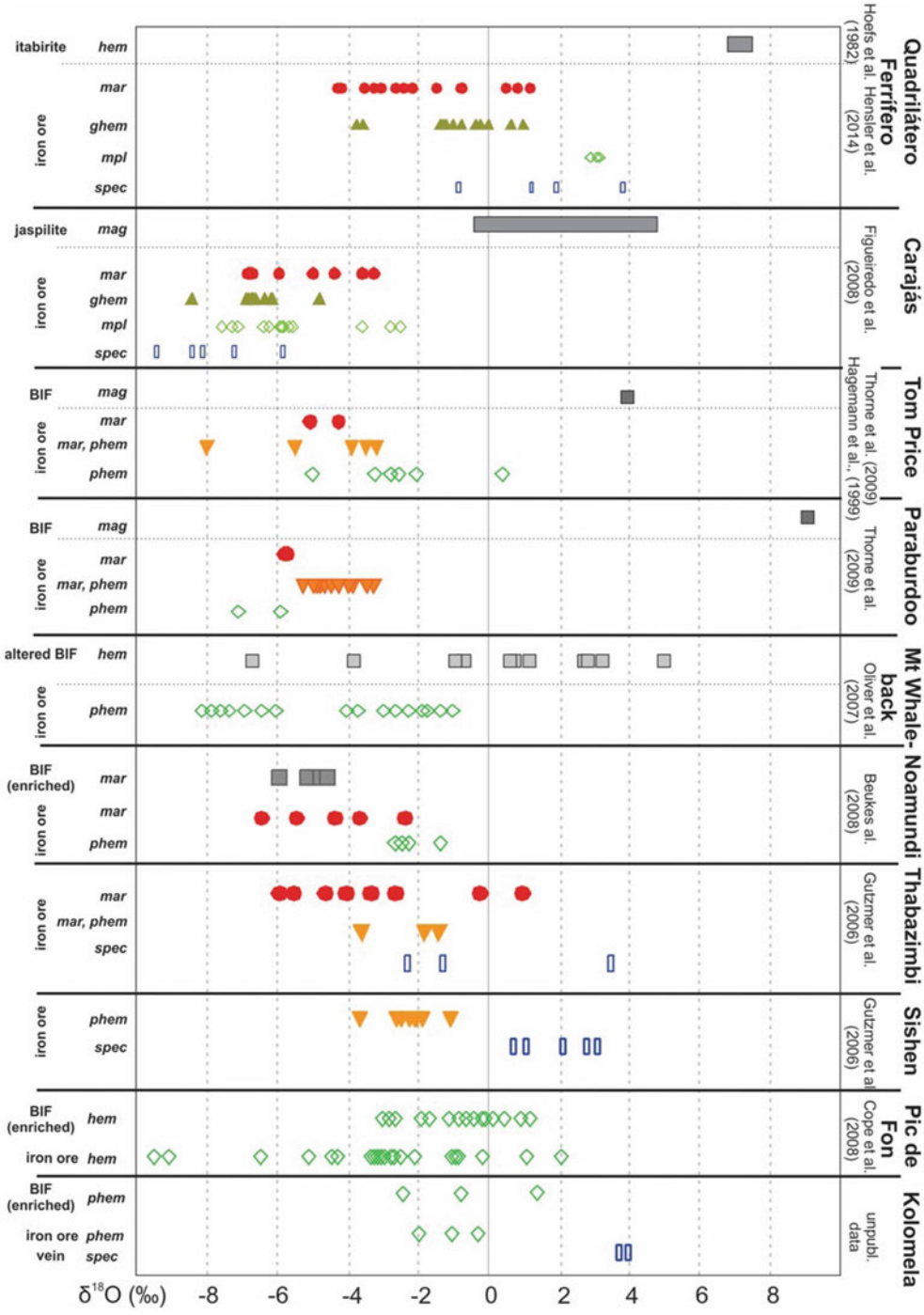

Fig. 2 Oxygen isotope values of different iron oxides (in ‰ relative to VSMOW) from various iron ore deposits worldwide (mag: magnetite, mar: martite, phem: platy hematite, mpl: microplaty hematite, spec: specular hematite) (modified after Hensler et al. 2014; Hagemann et al. 2016). Hematite oxygen isotope data from the Pic de Fon ore deposit were calculated on the basis of whole-rock and quartz oxygen isotope data (Cope et al. 2008). A depletion in ^{18}O from iron oxide of the least altered protore BIF/itabirite/jaspilite (grey box) to high-grade iron ore is documented in most ore deposits. Furthermore, across the paragenetic sequences of the Quadrilátero Ferrífero, Tom Price, Noamundi and Transvaal ores, earlier formed iron oxides (e.g. martite, granoblastic hematite) have mainly lower $\delta^{18}O$ values relative to later formed iron oxides (e.g. microplaty, platy and specular hematite)

hematite in the intermediate alteration zones and −8.3 to −5.8‰ and −6.7 to −4.3‰ for hematite from proximal alteration and high-grade martite-microplaty hematite ore, respectively (Thorne et al. 2004). Similar trends are observed at the Paraburdoo and Channar deposits (Fig. 2; Thorne et al. 2009).

The systematic decrease of $\delta^{18}O_{fluid}$ values from magnetite of the BIF to altered oxide-silicate-carbonate and to monomineralic oxide assemblages in the intermediate and proximal alteration zones, respectively, are interpreted by a variety of authors including Thorne et al. (2008), Angerer et al. (2014) and Hagemann et al. (2016) as evidence for the incursion of two hydrothermal fluids within the fault and shear zones. These fluids transformed BIF to high-grade iron ore via a series of complex fluid-rock reactions (cf. Hagemann et al. 2016). The ore-forming fluids are basinal brines ($\delta^{18}O_{fluid}$ values ranging between −2.0 and 6.0‰) and meteoric water ($\delta^{18}O_{fluid}$ values < −2‰).

Late-stage talc-bearing ore at the Mt. Tom Price deposit (Fig. 2) formed in the presence of a pulse of ^{18}O-enriched basinal brines, indicating that hydrothermal fluids may have repeatedly interacted with the BIFs during the Paleoproterozoic (Thorne et al. 2009).

Hydrothermal quartz-hematite veins from the Southern Batter fault zones within the Southern Ridge ore body at Tom Price show restricted $\delta^{18}O$ values for quartz from 16.1 to 18.3‰ (Hagemann et al. 1999). The $\delta^{18}O_{fluid}$ values were calculated using temperatures of 160 °C, estimated from microthermometric studies on the same quartz samples, and the quartz-H_2O fractionation curve (Matsuhisa et al. 1979); the $\delta^{18}O_{fluid}$ values range between −0.1 and 4.1‰. Hagemann et al. (1999) interpret these data as evidence for the influx of meteoric water or basinal brines that show minor fluid-rock reactions.

3.1.2 Spatial Distribution of $\delta^{18}O$ Values

At Mt. Tom Price there is a clear spatial relationship between the depletion in ^{18}O of hematite and magnetite relative to the BIF and the Southern Batter fault zone (Fig. 3). From a structural-fluid dynamic point of view the Southern Batter fault zone represents the main conduit for ascending and descending hydrothermal fluids in the Tom Price deposit (Hagemann et al. 1999; Taylor et al. 2001). The $\delta^{18}O$ values of samples proximal or within the Southern Batter fault zone are expected to be the most fluid dominated. For a given temperature their oxygen isotope compositions are likely to relate closely to those of the hydrothermal fluid, in this case meteoric water characterized by values from −8.6 to < 2‰ (Fig. 3). Farther from the fault zones, and at the periphery of the hydrothermal system, the $\delta^{18}O_{fluid}$ values of the iron oxides (−2 to 6.0‰) represent oxygen sourced from both the BIF and, to a lesser extent, the hydrothermal fluids.

Similar spatial zonation patterns were observed at Paraburdoo where $\delta^{18}O_{fluid}$ values of high-grade ore located within or close to the 4E Basal fault range between −9.6 and −6.0‰, whereas the proximal alteration zones bordering the fault zone display $\delta^{18}O_{fluid}$ between −0.9 and −0.6‰ (Thorne et al. 2009, 2014). The least altered Dales Gorge Member BIF display $\delta^{18}O_{fluid}$ values of 8.8 and 13.0‰ (Thorne et al. 2009, 2014).

3.1.3 Carbon and Oxygen Isotope Data on Carbonates

Detailed oxygen and carbon isotope analyses were performed on hydrothermally altered hematite-ankerite-magnetite in the North deposit, Tom Price (Thorne et al. 2004). Lower $\delta^{13}C$ values of ankerite ($\delta^{13}C$; −4.9 ± 2.2‰) from the hematite-ankerite-magnetite alteration zone, when compared to unmineralised BIF, indicate that the bulk of the carbon within the alteration zone is not derived from the BIF sequence (Thorne et al. 2004; Fig. 4). Similar oxygen isotope compositions, but increasingly heavier carbon isotopes from magnetite-siderite-iron silicate alteration (−8.8 ± 0.7‰) to hematite–ankerite–magnetite alteration zones (−4.9 ± 2.2‰), suggest the progressive exchange (mixing) with an external fluid with a heavy carbon isotope signature. It is likely that these saline

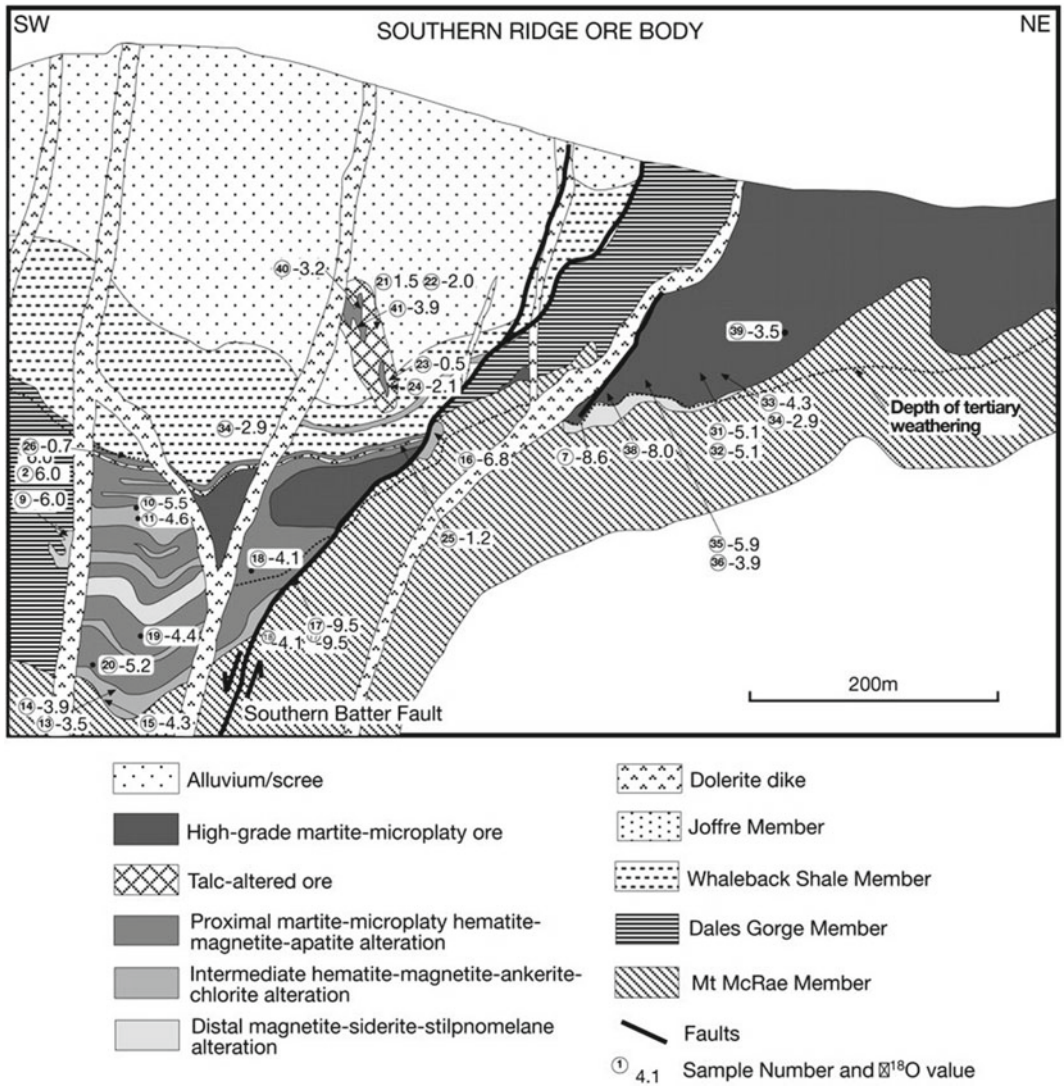

Fig. 3 Cross section of the Southern Ridge ore body at the Mt. Tom Price deposit displays the stratigraphic units and major normal faults, the spatial distribution of hydrothermal alteration assemblages and high-grade ore, and the $\delta^{18}O$ values (in ‰) of hematite and magnetite samples. Samples obtained from open-pit grab samples and diamond drill core. Note the low $\delta^{18}O$ values of samples proximal to fault zones. Section shown facing west. Reproduced with permission from Thorne et al. (2009); Copyright 2009 Society of Economic Geologists

fluids either reacted with the rocks from the Wittenoom Formation, or mixed with a fluid derived from the Wittenoom Formation (0.9 ± 0.7‰), and thus provided such a fluid composition (Fig. 4). Recent interpretation based on thermodynamic modelling of the de-silicification and carbonate addition processes at Tom Price questions the sole capacity of silica-dissolution of upward-flowing brines sourced from dolomite of the Wittenoom Formation, through shale-dominated Mt Sylvia and Mt McRae Formations (Evans et al. 2013). Instead, gravity-driven brines from an evaporitic source on an up-temperature pathway are a possible alternative solution to dissolve the large amount of chert required to form a giant hematite iron ore deposit such as at Mt. Tom Price (Evans et al. 2013). Likely, the de-silicification and carbonate

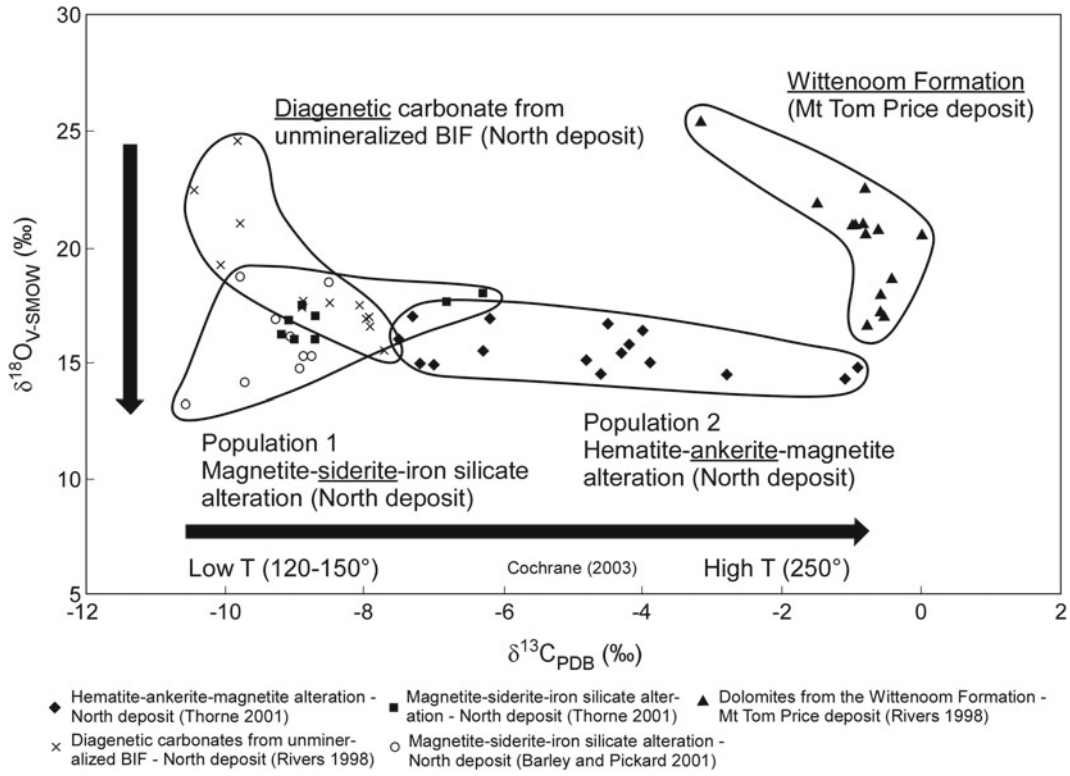

Fig. 4 Oxygen versus carbon isotope diagram showing the isotopic composition of diagenetic carbonates from unmineralised BIF, magnetite–siderite–iron silicate, hematite–ankerite–magnetite alteration and Wittenoom Formation in the Hamersley province, Western Australia. All samples are from the North deposit at the northern end of the Mt. Tom Price deposit, except from the Wittenoom Formation, which are from the Mt. Tom Price deposit. Temperatures of carbonate formation are obtained from Cochrane (2003). Modified after Thorne et al. (2014) and Hagemann et al. (2016).

addition processes in giant BIF-hosted deposits are complex and may contain both upwards and downwards flowing and/or possibly alternating, hydrothermal fluids.

Angerer et al. (2014) presents carbon and oxygen isotope data from early (co-magnetite) and late (co-specular hematite) carbonate generations documented at the Koolyanobbing, Beebyn and Windarling deposits in the Yilgarn craton (Fig. 5). The overall trend from heavy O and light C in early carbonate-magnetite stages to light O and heavy C in late carbonate-oxide stages is similar to the trends observed in the distinct alteration stages at the Mt. Tom Price deposit (Fig. 4; Taylor et al. 2001; Thorne et al. 2004; 2008; Angerer et al. 2014). The signature of the late-stage dolomite in Yilgarn deposits is compatible with the down flow of meteoric water and/or seawater into fault zones and associated ore bodies, assuming that $\delta^{13}C$ of Archean seawater is about 0‰, and that the O isotope signature of sea-/meteoric water remained constant during the hydrothermal process(es). The similarity of C and O isotope patterns between deposits in the Yilgarn (Fig. 5) and Hamersley province (Fig. 4) may be a coincidence, although at the least it suggests that contrasting processes and fluid sources can lead to similar isotopic values.

3.1.4 Hydrogen Isotope Data on Fluid Inclusions in Quartz

Hydrogen isotopes were obtained from fluid inclusions trapped in quartz from quartz-hematite veins of the Southern Batter fault zones in the Southern Ridge ore body at Tom Price. Fluid

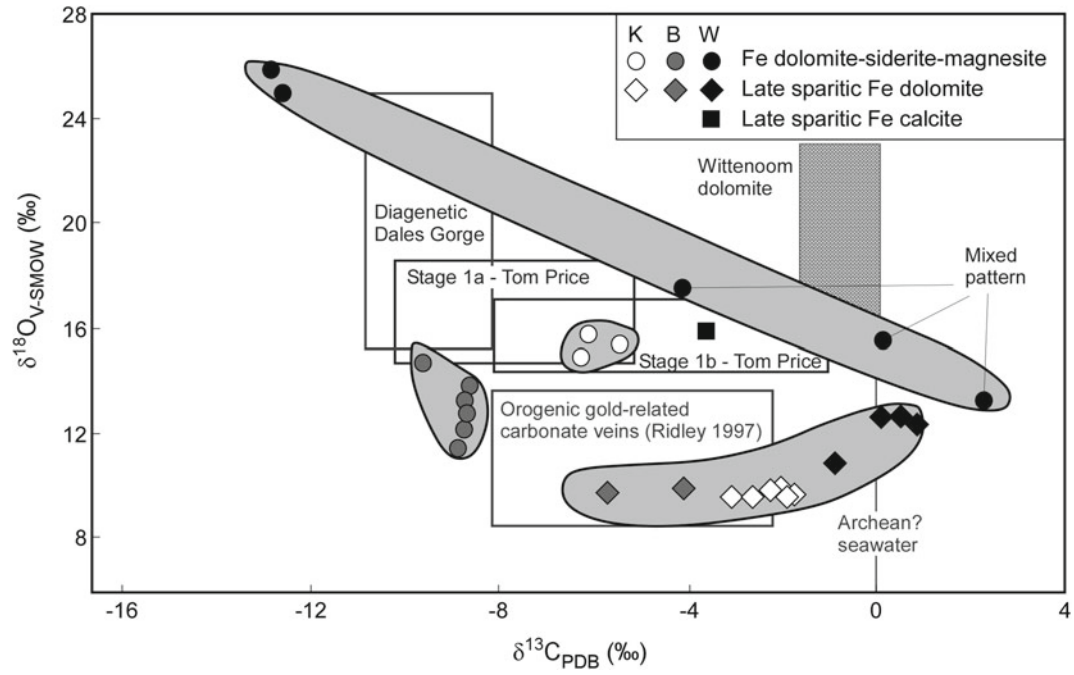

Fig. 5 Carbon and oxygen isotope data of hydrothermal carbonate in the Yilgarn craton deposits Koolyanobbing (K), Beebyn (B) and Windarling (W). Shown for comparison are data fields for diagenetic siderite/ankerite from the Dales Gorge BIF, hydrothermal ankerite from Tom Price stage 1a and 1b alteration zones, Paraburdoo Member of the Wittenoom dolomite (Taylor et al. 2001 and references therein), and carbonate veins in Yilgarn Craton orogenic gold deposits (Ridley 1997). Modified after Angerer et al. (2014)

inclusion waters yield a large range of δD values from −90‰ to −35‰ (Hagemann et al. 1999) with two populations at −53 to −66‰ and −34 to −43‰, and a single analysis of −90‰. These values were interpreted by Hagemann et al. (1999) as compatible with either seawater that was shifted to more negative values or, alternatively, with meteoric water or basinal brines that reacted with wallrocks.

3.2 Africa

3.2.1 Oxygen Isotope Data on Hematite

The majority of stable isotope data from South African BIF-hosted iron ores reported to date are essentially confined to bulk-rock measurements of massive hematite ore, irrespective of the textural variability of the ores. The general lack of carbonates in the ores and in adjacent rocks precludes them as targets for carbon and oxygen on carbonate isotope analyses. Limited data from early- and late-stage hematite from Thabazimbi have been reported by Beukes and Gutzmer (2008) and these are briefly referred to elsewhere in this paper when hydrothermal deposits are discussed in detail.

With respect to the predominant ancient-supergene type of ores at the Maremane Dome, the absence of systematic oxygen isotope studies is mainly due to the obvious lack of recognised alteration zones developed in BIF adjacent to the ores that would themselves provide potential first-order exploration vectors. Moreover, as indicated earlier, karst-hosted iron ore deposits at the Maremane Dome contain texturally diverse ore types across space, with a strong detrital component as encapsulated particularly in the breccia and conglomeratic ore types. In fact, pre-ore BIF may not be preserved at all in direct contact with some of these ore occurrences

(Moore et al. 2011). Such ores are invariably unsuitable for targeted sampling aimed at stable isotope analyses due to their inherently heterogeneous textural nature, and have thus led to the predominantly bulk sampling approach.

Figure 6 provides a comprehensive summary of oxygen isotope data for bulk hematite iron ore samples from three localities of ancient-supergene ore at the Maremane Dome of the Griqualand West area, namely Sishen, Beeshoek and Kolomela. The diagram also includes, for comparative purposes, data for the hydrothermal Thabazimbi ores from the Transvaal area. An obvious first observation on the diagram of Fig. 6 is the similarity in the range of $\delta^{18}O$ values for the supergene ores, between −4 and 3‰, with approximately two-thirds of the data falling in the range −4 to 0‰. Although the overall range in $\delta^{18}O$ values probably reflects the intrinsic sample heterogeneity behind the bulk ore measurements, the overwhelmingly light oxygen isotopic signature has been—and is being—used as strong indication for the meteoric character of the hydrothermal fluids implicated in ore formation and, by extension, for the paleo-supergene origin of the ores (Smith and Beukes 2016). The data range from the Thabazimbi ore is comparatively larger, with recorded $\delta^{18}O$ values as low as −6‰ and as high as 4‰. Interestingly, similar measured $\delta^{18}O$ values for hematite of the hydrothermal ores at Pic de Fon of Guinea also record a large range of low $\delta^{18}O$ between a maximum value of 1.3‰ and a minimum value of −8.9‰, suggestive of an ultimately paleo-meteoric source for the mineralising hydrothermal fluids.

Recent studies on altered BIF intersections adjacent to, and intercalated with, massive iron ore in the broader Kolomela area, have revealed several generations of microplaty to specular hematite veinlets and apparent replacement textures at the expense of the BIF (Papadopoulos 2016). Oxygen isotope data of micro-drilled hematite from such occurrences are included in Fig. 2. The data indicate that the vein and replacement type hematite records generally higher $\delta^{18}O$ values by comparison to adjacent massive hematite ore, and this is an observation that is in general agreement with similar signatures in hydrothermal ore types as discussed elsewhere in this paper. It is, therefore, possible that the iron ores at the Maremane Dome are not exclusively ancient-supergene in origin, and may contain a significant hydrothermal component to their formation, possibly in a fashion akin to supergene-modified genetic models.

Oxygen isotope data from the Simandou iron ore district of Guinea are solely obtained from the Pic de Fon deposit and can be categorised into two populations (Cope et al. 2008). Relatively higher values from least-altered BIF samples, when compared to BIF from the Hamersley or Kapvaal provinces, are interpreted to reflect fluid-rock interaction processes during retrograde, greenschist facies conditions. In contrast, samples of BIF that are significantly enriched in iron record a shift towards much lower $\delta^{18}O$ values (Fig. 2), comparable in their overall range to those from other hydrothermal iron ore deposits such as Thabazimbi (South Africa), Noamundi (India) and Mt. Tom Price (Australia). This is consistent with fluid-rock interaction involving large volumes of isotopically light, evolved meteoric water, at moderate temperatures (<380 °C). A slight decrease in the $\delta^{18}O$ values of coexisting quartz appears to conform to the same interpretation by virtue of its limited isotopic exchange with the same meteoric-sourced fluids.

3.3 Brazil

3.3.1 Oxygen Isotope Data on Iron Oxides

Oxygen isotope analyses across the complex iron oxide paragenetic sequence of the QF reveal distinct $\delta^{18}O$ signatures (Fig. 2: Hensler et al. 2014). With respect to the itabirite-hosted and ore forming iron oxide generations, differences in the oxygen isotope signature are particularly observed between the itabirite-hosted hematite, the early ore-forming iron oxides (martite and granoblastic hematite) and the late ore-forming iron oxides (microplaty and specular hematite). The $\delta^{18}O$ values of ore-hosted martite range

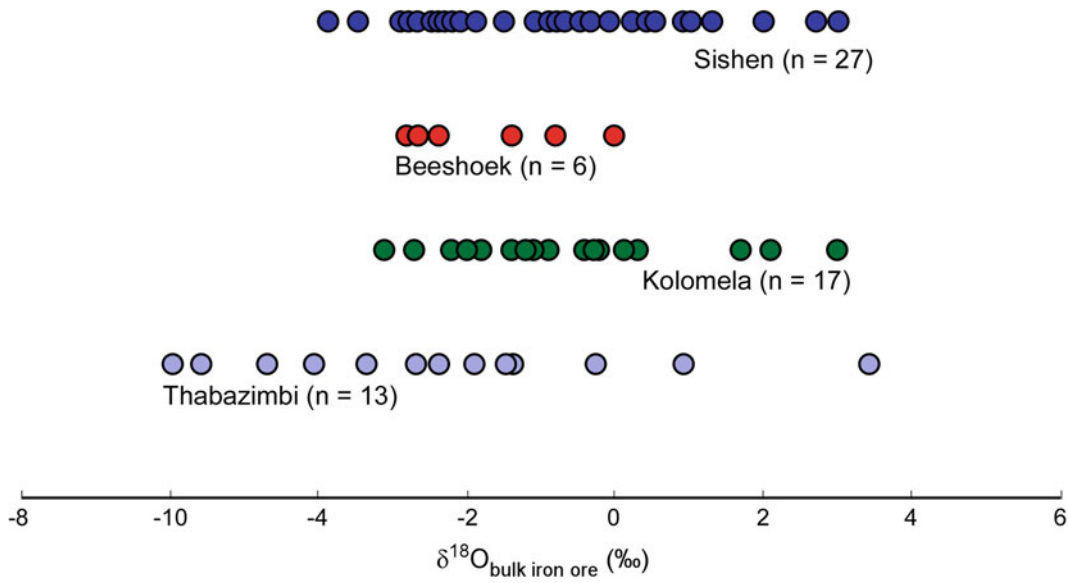

Fig. 6 Compilation of bulk hematite oxygen isotope data (versus VSMOW) for massive, laminated and breccia/conglomeratic-type iron ores of the Transvaal Supergroup, South Africa. The Sishen and Beeshoek deposits and the Kolomela prospect in the Griqualand West Basin represent examples of iron ore mineralisation of an ancient supergene origin. By contrast, the Thabazimbi deposit in the eastern Transvaal Basin is interpreted as hydrothermal in origin. Sishen data from Gutzmer et al. (2006); Beeshoek data from van Deventer (2009); Heuninkranz data from Land (2013) and Papadopoulos (2016); and Thabazimbi data from Netshiozwi (2002)

between −4.4 and 0.9‰ (Fig. 2) and are significantly depleted when compared to hematite from least-altered itabirite (~7‰: Hoefs et al. 1982). This strong depletion in ^{18}O is likely the result of the influx of large volumes of hydrothermal fluids with light ^{18}O signatures, and an extreme chemical fluid-rock exchange at low temperatures (<150 °C) and high fluid-rock ratios during the martitisation and cogenetic iron ore formation. The recrystallised ore-hosted granoblastic hematite has similar light $\delta^{18}O$ values compared to ore-hosted martite, ranging between −4.1 and 0.6‰ (Fig. 2). Similar $\delta^{18}O$ signatures of martite and granoblastic hematite assume that recrystallisation of granoblastic hematite took place under "isochemical" conditions with the martite, thus without major oxygen isotope exchange. This may be either due to the participation of only small fluid volumes and/or because the oxygen isotope composition of the fluid was in equilibrium with the earlier formed martite during recrystallisation. Relative to the early stage iron oxides (martite and granoblastic hematite), the later-stage microplaty and specular hematite that form the schistose ore have significantly heavier $\delta^{18}O$ values, ranging between 3.0–3.2‰ and −0.9–3.8‰, respectively (Fig. 2). This increase in the $\delta^{18}O$ values of the schistose, ore-forming hematite generations is likely to reflect the precipitation of microplaty and specular hematite from fluids with heavier oxygen isotope compositions during the later-stage of ore formation (Hensler et al. 2014). Interestingly, an increase in the $\delta^{18}O$ ratios from earlier stage hematite to later stage hematite is also recorded in other high-grade iron ore deposits worldwide, such as Noamundi, Thabazimbi, and Tom Price (Gutzmer et al. 2006; Beukes et al. 2008; Thorne et al. 2008, respectively).

Calculations of the $\delta^{18}O$ of fluids in equilibrium with the iron oxides of the QF were performed using the water-hematite curve after Yapp (1990) assuming temperatures of 145 °C (Rosière et al. 2008) for martite, granoblastic and microplaty hematite and at a temperature of 350 °C for specular hematite (Rosière et al.

2008). Fluids in equilibrium with martite and granoblastic hematite have relatively low average $\delta^{18}O_{fluid}$ values (approx. 0.8‰ and 1.6‰, respectively), whereas microplaty hematite and specular hematite have high average $\delta^{18}O_{fluid}$ values (6.0‰ and 9.6‰, respectively). With respect to the iron ore genesis and source of ore-forming fluids, the oxygen isotope compositions of the fluids in equilibrium with the distinct iron oxide paragenesis are interpreted to reflect: (i) the participation of isotopically light hydrothermal fluids (e.g. meteoric water or basinal brines) during the martitisation and likely cogenetic upgrade of itabirite to high-grade iron ore; and (ii) participation of modified meteoric water (with elevated $\delta^{18}O_{fluid}$ values) and/or infiltration of isotopically heavy fluids (e.g. metamorphic or magmatic water) into the ore system during the precipitation/crystallisation of microplaty and schistose specular hematite.

Figueiredo e Silva et al. (2008, 2013) selected samples for oxygen isotopes from the Carajás iron ores and least altered jaspilite from: (1) magnetite, (2) microplaty hematite, (3) anhedral hematite, (4) tabular hematite, (5) quartz from different vein breccias, and (6) least-altered (whole-rock basis) jaspilite containing the assemblage microcrystalline hematite ± martite; analyses of microcrystalline hematite were also performed. The $\delta^{18}O$ values display a large range (Fig. 2) from 15.2‰ for the least-altered jaspilites (whole-rock analyses; not shown in Fig. 2) to −9.5‰ for the paragenetically latest, euhedral-tabular hematite (Fig. 2) in the high-grade iron ore. The $\delta^{18}O_{fluid}$ values were calculated based on: (1) homogenization temperatures, after pressure correction, of fluid inclusions trapped in quartz and carbonate crystals that are in textural equilibrium with hematite and/or magnetite (Figueiredo et al. 2008, 2013; Lobato et al. 2008), and (2) the fractionation factors of Yapp (1990) for hematite, Zheng (1991, 1995) for magnetite, and Matsuhisa et al. (1979) for quartz. For magnetite, the average pressure-corrected trapping temperature of 245 °C, obtained from microthermometry analyses of fluid inclusions within vein type 1 quartz-carbonate crystals that are in textural equilibrium with magnetite, was used. For hematite, trapping temperatures (245–285 °C) of fluid inclusions trapped in rare quartz in equilibrium with hematite were used. The $\delta^{18}O_{fluid}$ values for the different hematite types increased about 6 to 8‰ with respect to the least altered jaspilite, whereas the average $\delta^{18}O_{fluid}$ value for magnetite increased by about 6‰ compared to the respective $\delta^{18}O$ values. There is a clear decrease in both the $\delta^{18}O_{fluid}$ and $\delta^{18}O_{fluid}$ values from the paragenetically earliest to the latest hematite types.

Oxygen isotope data on iron ore of the Urucum mining district have been performed on whole-rock banded iron ores, because mineral separation was not feasible due to diminutive hematite grain sizes (Hoefs et al. 1987). Calculations of the isotopic compositions of the two minerals comprising the BIF (namely hematite and quartz; Hoefs et al. 1987) reveal $\delta^{18}O$ values ranging between 21.3 and 26.4‰ for quartz and 0.8 to 6.5‰ for hematite. Temperature calculations using different hematite-quartz fractionation curves (Blattner et al. 1983; Matthews et al. 1983) propose that hematite (and quartz) crystallised at temperatures between 250 °C and 280 °C, and that the involved fluid had a $\delta^{18}O_{fluid}$ composition above 10‰ (Hoefs et al. 1987). With respect to the exceptional high oxygen isotopic fluid compositions, Hoefs et al. (1987) interpret that the isotopic composition of the iron ore reflect the diagenetic and burial metamorphic conditions, that have largely obliterated primary depositional oxygen isotope signatures of the BIF quartz and hematite. In a later study, Yapp (1990) used the same oxygen isotope data from the Urucum mining district that were originally published by Hoefs et al. (1987) in order to calculate the depositional temperatures of the Urucum BIF and related $\delta^{18}O_{fluid}$ values using the hematite–water and quartz-water fractionation curves of Yapp (1990) and Knauth and Epstein (1976), respectively. In contrast to the relatively high crystallisation temperatures of Hoefs et al. (1987), the calculated depositional temperatures (Yapp 1990) are low (ranging between 0 and 35 °C) and oxygen isotope signatures of involved fluids range between −8.8 and 0.0‰. Yapp (1990) interpreted this data as

an oxygen isotope signature that reflects the primary glaciogene environment present during the BIF deposition rather than an overprint and modification of earlier isotopic signatures by post-depositional processes.

Using the isotopic composition of reworked rocks for the investigation of their depositional conditions assumes that isotopic exchange during diagenesis/metamorphism was negligible and that the primary isotopic composition was preserved during the diagenesis/metamorphism of the rocks.

3.3.2 Carbon and Oxygen Isotope Data on Carbonates

Except one recently published carbon isotope study by Figueiredo e Silva et al. (2013), that was carried out on hydrothermal BIF-hosted carbonates of the Carajás mining province, most of carbon and oxygen isotope data on carbonates from Brazilian BIF-hosted ore (e.g. from the QF and Urucum) have been performed on (least-altered) BIFs/itabirite in order to gain information about the depositional conditions and environment during which the BIFs were formed and not to track post-depositional alteration and ore genetic processes. Importantly, in order to allow a conclusion to what extent carbon and oxygen isotope signature at the QF and Urucum may reflect post-depositional alteration and ore genetic processes, detailed carbon and oxygen isotope studies need to be conducted also on highly altered (e.g., hydrothermal carbonate) and iron enriched BIF ore.

Detailed carbon and oxygen isotope data (Spier et al. 2007) on carbonates from the Cauê dolomitic itabirite sequence of the Águas Claras deposit reveal negative $\delta^{13}C$ values ranging between −2.5 and −0.8‰ and $\delta^{18}O$ values ranging between −8.5 and −2.4‰. Similar $\delta^{13}C$ values have been obtained in another carbon and oxygen isotope study on the carbonate-rich itabirites of the Aguas Claras deposit (Morgan et al. 2013), which reveal $\delta^{13}C$ values between −1.6 and 2.4‰. Respective $\delta^{18}O$ values differ from the study of Spier et al. (2007) ranging between −14.4 and −10.2‰. These differences in the $\delta^{18}O$ composition in the study by Spier et al. (2007) and Morgan et al. (2013) may be attributed to different sample locations within the Aguas Claras deposit and, accordingly, to a different mineralogical content of the analysed samples. In fact, Morgan et al. (2013) reports the $\delta^{18}O$ values becoming less negative with increasing depth, which may be related to different degree of weathering of the analysed samples. However, Spier et al. (2007), as well as Morgan et al. (2013), interpreted the $\delta^{13}C$ (and partially also the $\delta^{18}O$) signatures of the QF itabirite to represent typical primary isotopic signatures of marine carbonates, which precipitated in a shallow marine environment from a seawater-hydrothermal fluid.

With respect to the Urucum mining district, carbon isotopic analyses have been carried out on carbonates from BIF, Mn-rich ore zones and carbonate-rich veinlets in Mn ore (Klein and Ladeira 2004) and further on dolomite-chert-hematite BIF of the Santa Cruz deposit (Angerer et al. 2016). The results show relatively homogenous negative $\delta^{13}C$ values ranging between −7.0 and −3.4‰ and are interpreted to reflect the typical glaciomarine environment in which the BIFs were deposited during Neoproterozoic times (Klein and Ladeira 2004; Angerer et al. 2016). The primary depositional carbon isotopic signature of the Neoproterozoic BIFs of the Urucum mining district has, therefore not been obliterated by post-depositional alteration and/or ore-forming fluids.

For the case of Carajás, carbonate samples were selected from different hydrothermal vein breccia types located mainly in the N4E deposit (Figueiredo e Silva et al. 2013) and consist of: (1) calcite and kutnahorite in discordant V1 veins located in the distal alteration zone within jaspilites; (2) kutnahorite and dolomite in V4 breccias in high-grade ore, with kutnahorite in textural equilibrium with an assemblage of martite and microplaty hematite; (3) calcite from amygdaloidal basaltic wallrock; and (4) calcite veins in hydrothermally altered basaltic wallrocks. Calcite-kutnahorite $\delta^{13}C$ and $\delta^{18}O$ values from the distal alteration zones show a large $\delta^{13}C$ range of −5.5 to −2.4‰, and a relatively narrow $\delta^{18}O$ range of 9.3 to 11.7‰. However, dolomite

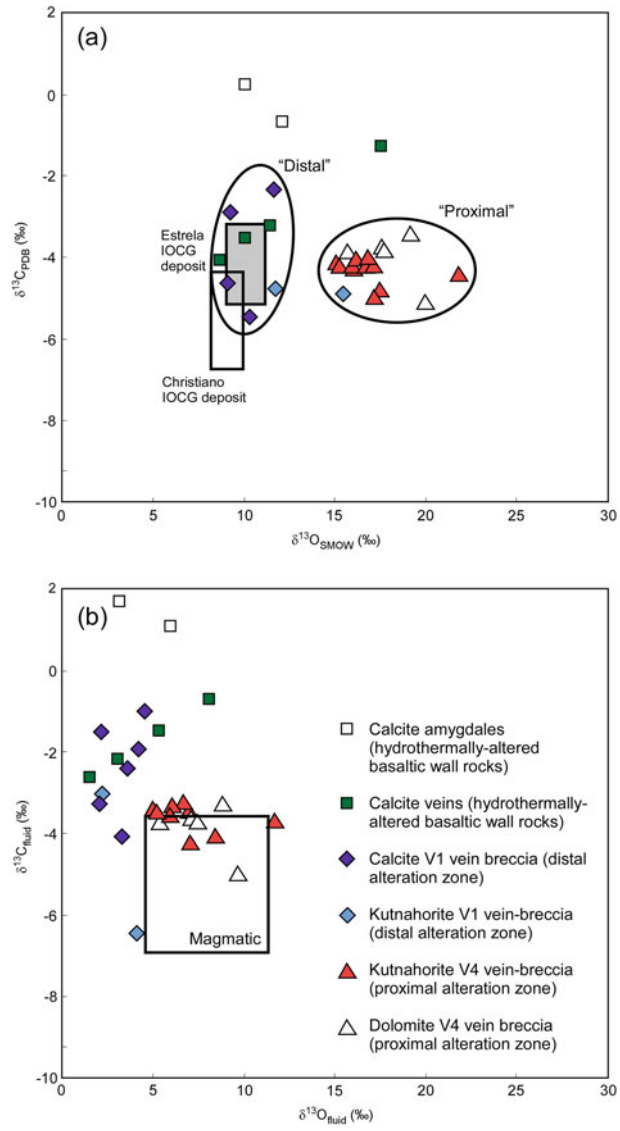

Fig. 7 Carbon and oxygen isotopes compositions of carbonates in calcite amygdale from the hydrothermally basaltic wall rock; calcite veins from distal alteration zone of basaltic wall rocks; calcite, kutnahorite from V1b vein-breccia in distal alteration zone in altered jaspilites, and dolomite and kutnahorite from V4 vein-breccia in proximal alteration zone. Symbols shown in (b) are also valid for (a). The two circles in (a) correspond to distal and proximal alteration zones, respectively; also shown are fields of oxygen and carbon isotopic composition of calcite from the Paleoproterozoic Cu (Mo–Au–Sn) Estrela deposit (Lindenmayer et al. 2005) (box in grey), and the Archean Cu(Au) Cristalino deposit (Ribeiro et al. 2007) (empty box).
b Diagram showing calculated carbon and oxygen fluid values based on trapping temperatures based on fluid inclusions studies. Magmatic field according to Kyser and Kerrich (1990)

matrix breccias from the advanced hydrothermal zone, *i.e.,* ore, exhibit a wider $\delta^{18}O$ range from 15.1 to 21.8‰ and a more restricted $\delta^{13}C$ range from −5.0 to −3.9‰ (Fig. 7). This latter ranges point to a single carbon source of possible magmatic nature, whereas the larger $\delta^{18}O$ range suggests multiple oxygen sources.

3.3.3 Hydrogen Isotope Data on Fluid Inclusions

Hydrogen isotope data were obtained from fluid inclusions trapped in quartz from hydrothermal V1a, V2 and V3 vein types in the Serra Norte iron deposits, Carajás (Fig. 8). The hydrogen values from fluid inclusions trapped in V2 and V3 quartz veins are interpreted to reflect fluids synchronous with iron mineralization and are restricted to −20 to −43‰ with two outliers at −3 and −104‰ (Fig. 8).

3.3.4 Oxygen Isotope Data on Silicates and Oxides

Oxygen isotope analyses of iron oxides of the Noamundi mining area were performed on

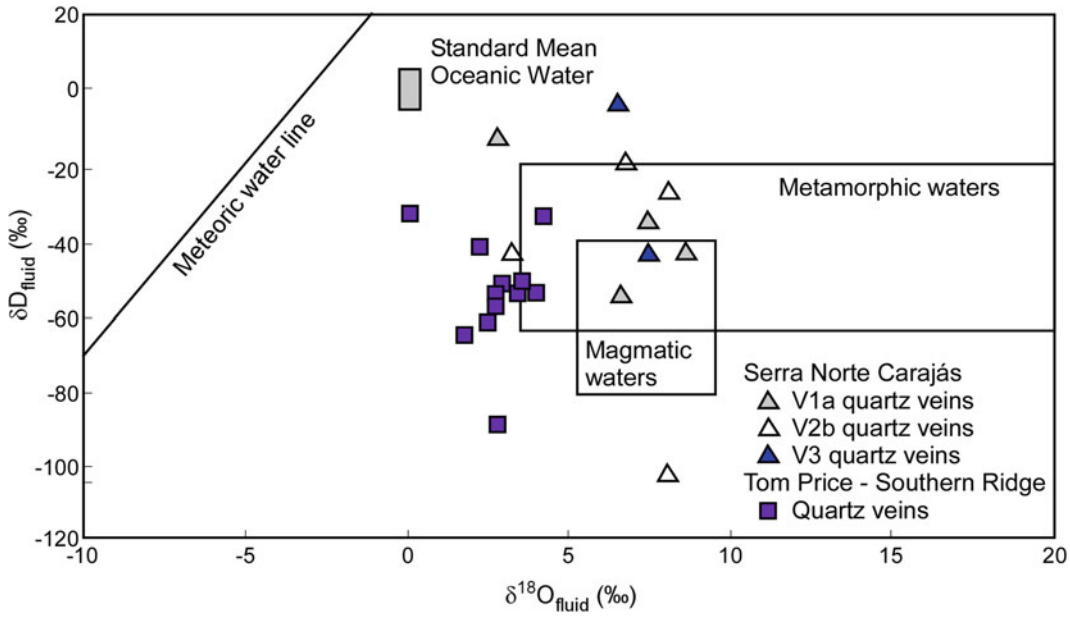

Fig. 8 Diagram displaying calculated $\delta^{18}O_{fluid}$ and δD isotope value for quartz and fluid inclusions, respectively from the Serra Norte iron deposits. Also presented are data from the Southern Ridge deposit at Tom Price in the Hamersley Province of Western Australia (Hagemann et al. 1999). The meteoric water line (Craig 1961), and fields of typical magmatic waters (Ohmoto 1986) and metamorphic waters as defined by Taylor (1974) are also shown.

cryptoplaty hematite from the hard iron ore and martite from partly mineralised BIFs and ore (Beukes et al. 2008). The oxygen isotope signature of cryptoplaty hematite ranges between −1.3 and 2.5‰. Relative to the ore-hosted cryptoplaty hematite, martite from the mineralised BIF and massive iron ore is depleted in ^{18}O and has $\delta^{18}O$ values ranging from −5.8 to −4.4‰ and from −6.7 to −2.6‰, respectively. The depleted $\delta^{18}O$ values of martite compared to cryptoplaty hematite is interpreted to reflect the formation of magnetite (as precursor mineral of martite) under higher temperatures than cryptoplaty hematite and a probable chemical inheritance of the oxygen isotope signature in martite from the magnetite precursor (Beukes and Gutzmer 2008). Additional interpretations about e.g. ore-forming fluid characteristics and sources have not been done so far by the means of the published oxygen isotope data (Beukes and Gutzmer 2008).

4 Interpretation of Oxygen, Carbon and Hydrogen Isotope Data with Respect to Hydrothermal Fluid Source(s), Fluid Flow and Processes

Oxygen and carbon isotope analyses on precursor BIF or, locally low-grade iron ore, have been completed since the early 1970's with landmark papers by Becker (1971), Clayton et al. (1972) and Becker and Clayton (1976) on carbon and oxygen isotope ratios on BIF in the Hamersley of Western Australia. The first study on specifically iron ore was by Hoefs et al. (1982) who investigated oxygen isotope signatures on selected iron ore from the QF in Brazil. It was not until the end of the 1990's that Hagemann et al. (1999) and Powell et al. (1999) reported oxygen isotopes on specific iron ore types from Hamersley

iron deposits, and then Gutzmer et al. (2006) published a now seminal paper on oxygen isotopes of hematite and the genesis of high-grade BIF-hosted iron ores from a variety of deposits in South Africa, Brazil, India, and Australia.

These early studies were then followed up with detailed oxygen and carbon isotope investigations on iron oxides (both magnetite and hematite) formed during specific paragenetic ore stages in both the hypogene and supergene environment. Whereas the early oxygen isotope studies solely concentrated on the origin of the precursor BIF, the investigations at the end of the 1990's and thereafter also focused on the origin of the iron ore with respect to their crustal position, i.e., whether these ores are the product of hypogene hydrothermal alteration and/or weathering and supergene enrichment. In addition, other studies used the stable isotope (oxygen and carbon isotopes) signatures of iron ore and gangue carbonate to develop deposit-specific fluid flow paths and hydrothermal models for the origin of BIF-hosted iron ore.

With respect to the hydrogen isotope, only limited data is available, and only from fluid inclusions trapped in quartz veins. It is important to point out that hydrogen data may overlap both the magmatic and metamorphic fluid reservoirs, making these isotopic signature alone non-diagnostic.

The following sections will summarize the fundamental contributions of stable isotopes in the genesis of BIF-hosted iron ore but also provide a summary of the implications for the origin of iron ore in specific iron ore districts throughout the world.

4.1 Stable Isotope Analyses and Genetic Implications

Before about 1990's the most widely accepted BIF-hosted iron ore model was a combination of pure supergene enrichment via deep weathering processes during the Mesozoic to Paleogene (e.g. Dorr 1964) and diagenetic and metamorphic dehydration of Paleoproterozoic goethite via downwards penetration of supergene fluids up to the base of weathering, i.e., the classic CSIRO-AMIRA supergene-metamorphic model (Morris 1985). At the end of the 1990's these models were then challenged by the results of stable isotope and fluid inclusion studies on iron oxides and gangue minerals such as carbonates and quartz, which allowed the detection and quantification of a variety of hydrothermal fluids including basinal brines (Hagemann et al. 1999; Thorne et al. 2004), magmatic fluids (Figueiredo e Silva et al. 2008) and ancient meteoric waters (Hagemann et al. 1999; Thorne et al. 2004; Figueiredo e Silva et al. 2008; Cope et al. 2008). Much of the renewed interest in the genesis of BIF-hosted iron ore was sparked by the availability of deep diamond cores, intercepting fresh, hypogene iron ore, carbonates and quartz well beneath the weathering horizon, which required a re-think of the accepted geological models of the time. It was at this time that the application of stable isotopes, in combination with fluid inclusions, revealed fundamental new data and allowed new interpretations on the origin of BIF-hosted iron ore. Some of the fundamental new interpretations included:

1. The large spread of the oxygen isotope composition in iron oxides, in all of the deposits that have been analysed to date, and a general depletion of ^{18}O from BIF-hosted to iron ore-hosted iron oxides suggests the involvement of meteoric water ($\delta^{18}O_{fluid}$ between −10 and 2‰) at the time of mineralisation, i.e. during the upgrade of BIF to iron ore.
2. The presence of $\delta^{18}O_{fluid}$ data > 4‰ suggest the involvement of an additional hydrothermal fluid, besides meteoric water, which was determined to be of magmatic nature in the case of the greenstone belt-hosted Carajás-type iron ore deposits and basinal brines in the case of the sedimentary basin-hosted Hamersley-type deposits.
3. The spread in carbon isotope data indicates that carbon is not necessarily derived from carbonate-rich BIF units but also contains a component of "external" carbon; in the case of the Carajás deposit magmatic carbon, in the case of the Hamersley deposits sedimentary carbon from the underlying Wittenoom

dolomite, and in the case of Yilgarn deposits surface water (either seawater or meteoric water).

4.2 Regional Interpretations

Where stable isotope analyses on oxides or quartz associated with iron ore were conducted, the results played a significant role in the identification of hydrothermal fluid types and in the interpretation of fluid flow models for the respective iron ore deposits.

In the itabirite-hosted iron ore of the QF, two major trends are observed: (1) iron oxides that form the high-grade iron ore have lower $\delta^{18}O$ values than iron oxides from the protore itabirite; and (2) across the ore-forming paragenetic iron oxide sequence, a minor increase in the $\delta^{18}O$ values is recorded. Hensler et al. (2014) suggested that the strong decrease in $\delta^{18}O$ values is likely related to the influx of large volumes of meteoric water, with light oxygen isotopic signature, during the upgrade of itabirite to iron ore. The same interpretation is favoured for the Pic de Fon deposit in West Africa, where iron-enriched BIF records a substantial shift towards low $\delta^{18}O$ values compared to least-altered BIF (Cope et al. 2008). The development of large "feeder" systems, such as shear and fault zones, is likely fundamental for the circulation of those large fluid volumes and, therefore, for the significant geochemical processes (e.g. de-silicification and oxidation of magnetite to martite) during the formation of high-grade iron ore bodies. With respect to the iron ore, the minor increase of $\delta^{18}O$ values from paragenetically earlier to later iron oxides, thus from martite and granoblastic hematite to microplaty and specular hematite, may reflect the participation of an oxygen isotopic heavier water (e.g. modified heavier meteoric, metamorphic, or magmatic water) during the iron ore modification.

The large Tom Price and Paraburdoo iron ore deposits display a similar oxygen isotope trend (Fig. 2) as recorded in the QF and the Pic de Fon deposit, thus a strong $\delta^{18}O$ decrease from BIF-hosted magnetite to ore-hosted hematite. Meteoric water likely played also a significant role in shifting the $\delta^{18}O_{fluid}$ values of up to 8.5‰ for magnetite in unaltered BIF to as low as −8.9‰ for martite and platy hematite in high-grade iron ore of Tom Price, Paraburdoo and Pic de Fon (Thorne et al. 2014; Cope et al. 2008). Oxygen and hydrogen isotopes on quartz, hematite and fluid inclusions, respectively from the Southern Batter fault zone in the Southern Ridge deposit also show significant negative $\delta^{18}O_{fluid}$ values for quartz and hematite (up to −4‰) and, when paired with the hydrogen values, suggest significant surface water influx (likely meteoric water) into the fault zone and ore body (Hagemann et al. 1999). In the giant Carajás Serra Norte iron ore deposits there is a systematic decrease in $\delta^{18}O$ values of oxides from early to late paragenetic stages (Fig. 2), indicating a progressive increase in the influx of isotopically light, meteoric waters with time and proximity to the high-grade, hard-iron orebodies (Figueiredo e Silva et al. 2013). Figure 8 displays $\delta^{18}O_{fluid}$ versus δD isotope values for quartz and fluid inclusions, respectively. Some data points from the Serra Norte iron ore deposits fall within the field of primary magmatic fluids (Taylor 1974), with two samples that shifted the isotopic values towards lighter $\delta^{18}O$ and heavier δD compared to those that characterise average magmatic fluid. This shift may indicate an uncertain amount of meteoric water influx into the mineral system and subsequent fluid-rock reactions. Values of quartz samples from the Southern Ridge iron ore deposit in the Hamersley Province in Western Australia (Hagemann et al. 1999) are also shown in Fig. 8, and clearly display different populations in δD and $\delta^{18}O_{fluid}$ relative to Carajás, suggesting different fluid sources and/or fluid-rock reactions for these two datasets. Most of the Carajás data points fall within the magmatic/metamorphic water boxes, whereas the majority of the Southern Ridge data plot outside these boxes. The lack of lower ^{18}O values towards the meteoric water line in the Carajás samples could be explained by the absence of data from late-stage quartz veins (proximal alteration zone), which better reflect the influx of meteoric water.

Also, interestingly, the Carajás hydrogen isotope data set is more restricted than that for the Hamersley iron deposits (Hagemann et al. 1999; Fig. 8), suggesting that basinal brines were not involved (Figueiredo e Silva et al. 2008).

5 Implications for Exploration of BIF-Hosted Iron Ore Systems

The decrease of $\delta^{18}O$ values in iron oxides from the distal to proximal alteration zone including the orebody may be used as a geochemical vector and provides a potential exploration tool particularly for finding high-grade iron ore deposits (e.g. in the QF), in which hematite/magnetite are frequently the only mineral that can be readily analysed. In combination with magnetic and gravity imaging this geochemical vector may assist in the identification of extensions of existing iron orebodies and in finding new, deep-seated concealed iron ore mineralisation. The mapping and identification of major structural pathways, which facilitate the circulation of large volumes of meteoric water commonly reflected by light oxygen isotope values, will be crucial for identifying itabirite that is upgraded to high-grade iron ore.

The systematic decrease in $\delta^{18}O$ values of oxides from BIF-to iron ore-hosted iron oxides indicates a progressive increase in the influx of isotopically light, meteoric waters with time and proximity to the high-grade, hard iron orebodies.

6 Limitations and Problems of Stable Isotope Analyses on BIF-Related Iron Ores

One of the overarching features of BIF-hosted iron ores globally, irrespective of their exact genetic origin (i.e. entirely supergene versus mixed hypogene-supergene), is the relatively large range in $\delta^{18}O$ data recorded in the iron oxide fraction. This is particularly seen in bulk-ore hematite isotopic data, suggesting that large variations in $\delta^{18}O$ are probably the result of analyses of highly heterogeneous mixtures of multiple iron oxide generations. Such data are likely to obscure rather than illuminate the origin of the ores and their spatial and temporal development. Nevertheless, in general, lowest $\delta^{18}O$ values in iron oxides characterise the most enriched portions of the ores, and this appears to apply both in some mixed hypogene-supergene deposits (e.g. Pic de Fon) and in those interpreted to have formed by ancient supergene processes only (e.g. Sishen). By contrast, hydrothermally altered BIF adjacent to the massive ores contains often texturally discrete generations of hematite (e.g. specular, microplaty) that also display heavy oxygen isotopes. This evident isotopic trend may be associated with either multiple fluids (e.g. evolved meteoric fluids versus basinal brines) involved in iron remobilisation and enrichment during the complex history of the deposits, and/or isotopic exchange reactions in structurally-controlled, largely single-fluid systems under progressively different fluid/rock ratios and temperatures.

Irrespective of the causes for the isotopic variations in space within a given deposit or prospect, it is crucial to be able to constrain and ensure as much as possible the integrity of the stable isotope data obtained. In classic mixed hypogene-supergene deposits such as those of the Hamersley basin, a multi-isotopic approach (O, C, H) on different mineral species (oxides, carbonates and silicates) combined with fluid inclusion investigations has been demonstrated to provide robust enough constraints on the nature of the hydrothermal system and its development in space (e.g. Thorne et al. 2008). This approach, however, is limited with respect to carbon isotope analyses in supergene-only deposits, which are also typically carbonate-destructive.

The great majority of BIF-hosted deposits are of hybrid origin (i.e. hypogene ore overprinted by modern supergene enrichment or modified ancient supergene-only ores). These likely record a large variety of textural forms of iron oxides on an equally large variety of scales, both in the massive ores and in associated altered BIFs. Isotopic analyses of minerals from these ores, in the absence of rigorous petrographic and textural analysis and documentation of detailed paragenetic stages are likely to produce biased and

misleading results. One must, therefore never underestimate the importance of detailed field work, petrography and mineral chemistry as the essential "backbone" of sound sample selection and robust geochemical and isotopic application in iron-ore exploration campaigns.

7 Conclusions

Stable oxygen and carbon isotope analyses in oxides, quartz and carbonate have significantly influenced the models for BIF-hosted iron ore worldwide.

Carbon and oxygen isotopes in carbonate associated with carbonate-rich, unaltered BIF and hydrothermal alteration carbonate suggest that $\delta^{13}C$ and $\delta^{18}O$ values of carbonates shift significantly from heavy to light $\delta^{13}C$ and light to heavy $\delta^{18}O$ values during hydrothermal alteration and mineralisation processes, thus suggesting an external (to the BIF) carbon source. Oxygen isotope studies on iron oxides from different ore deposits worldwide display a major decrease in the $\delta^{18}O$ values from BIF- to iron ore-hosted oxides and display the circulation and significance of large volumes of light oxygen isotope meteoric water during the upgrade of BIF to high-grade iron ore. Exploration of hidden BIF-hosted iron ore or extension of known iron ore bodies can be significantly assisted with stable isotope analyses of oxides, quartz and carbonate. Significant shifts in $\delta^{18}O$ and $\delta^{13}C$ values likely indicate massive hydrothermal fluid flow in the direction of high permeability fault zones, which in many deposits coincide spatially with zones of high-grade iron ore.

Acknowledgements The authors acknowledge David Huston who invited us to prepare this paper. This scientific work would have not been possible without the generous support of various mining and exploration companies including Rio Tinto, BHP, Atlas Iron, Vale, Vallourec, Kumba and Vectra. HT also likes to acknowledge `ASSMANG Ltd' for their past and ongoing support of the iron ore research group at Rhodes University. SGH, AH and RFS also thank Carlos Alberto Rosière, Phil Brown, Thomas Angerer and Paul Duuring for many stimulating discussions. SGH, AH and RFS also thank Lydia Lobato for many insightful discussions at the Lobato headquarters.

References

Angerer T, Duuring P, Hagemann SG, Thorne W, McCuaig TC (2014) A mineral system approach to iron ore in Archaean and Palaeoproterozoic BIF of Western Australia. Geol Soc London Spec Publ 393:81–115

Angerer T, Hagemann SG, Walde DHG, Halverson GP, Boyce AJ (2016) Multiple metal sources in the glaciomarine facies of the Neoproterozoic Jacadigo iron formation in the "Santa Cruz deposit", Corumbá, Brazil. Precambrian Res 275:369–393

Basson IJ, Koegelenberg C (2017) Structural controls on Fe mineralization at Thabazimbi Mine, South Africa. Ore Geol Rev 80:1056–1071

Becker RH (1971) Carbon and oxygen isotope ratios in iron-formation and associated rocks from the Hamersley Range of Western Australia and their implications. Unpublished PhD thesis, University of Chicago

Becker RH, Clayton RN (1976) Oxygen isotope study of a Precambrian banded iron formation, Hamersley Range, Western Australia. Geochim Cosmochim Acta 40:1153–1165

Beukes NJ, Gutzmer J (2008) Origin and paleoenvironmental significance of major iron formations at the Archean-Paleoproterozoic boundary. Rev Econ Geol 15:5–47

Beukes NJ, Gutzmer J, Mukhopadhyay J (2003) The geology and genesis of high-grade iron ore deposits. Trans Inst Mining Metall Sect B 112:B1–B25

Beukes NJ, Mukhopadyay J, Gutzmer J (2008) Genesis of high-grade iron ores of the Archean Iron Ore Group around Noamundi, India. Econ Geol 103:365–386

Bhattacharya HN, Ghosh KK (2012) Field and petrographic aspects of the iron ore mineralizations of Gandhamardan Hill, Keonjhor, Orissa and their genetic significance. J Geol Soc India 79:497–504

Blattner P, Braithwaite WR, Glover RB (1983) New evidence on magnetite oxygen isotope geothermometers at 175° and 112 °C in Wairakei steam pipelines (New Zealand). Chem Geol 41:195−204

Cabral AR, Rosière CA (2013) The chemical composition of specular hematite from Tilkerode, Harz, Germany: implications for the genesis of hydrothermal hematite and comparison with the Quadrilátero Ferrífero of Minas Gerais, Brazil. Miner Deposita 48:907–924

Clayton RN, O'Neil JR, Mayeda TK (1972) Oxygen isotope exchange between quartz and water. J Geophys Res 77:3057–3067

Cochrane N (2003) Phosphorus behavior during banded iron-formation enrichment. Unpub BSc thesis, University of Queensland, 86 p

Cope IL, Wilkinson JJ, Boyce AJ, Chapman JB, Herrington RJ, Harris CJ (2008) Genesis of the Pic de Fon iron oxide deposit, Simandou Range, Republic of Guinea, West Africa. Rev Econ Geol 15:197–222

Craig H (1961) Isotope variations in meteoric waters. Science 133:1702–1703

Dalstra HJ (2006) Structural controls of bedded iron ore in the Hamersley Province, Western Australia—an example from the Paraburdoo Ranges. Trans Inst Mining Metall Sect B 115:B139–B140

DNPM (2005) Brazilian Mineral Yearbook 2005:512, Brasilia, (DNPM)

Dorr JVN (1964) Supergene iron ores of Minas Gerais, Brazil. Econ Geol 59:1203–1240

Duuring P, Angerer T, Hagemann G (2017a) Iron ore deposits of the Yilgarn craton. Austr Inst Mining Metall Mon 32:181–184

Duuring P, Teitler Y, Hagemann SG (2017b) Iron ore deposits in the Pilbara craton. Austr Inst Mining Metall Mon 32:345–350

Evans K, McCuaig T, Leach D, Angerer T, Hagemann S (2013) Banded iron formation to iron ore: a record of the evolution of Earth environments? Geology 41:99–102

Figueiredo e Silva RC, Lobato LM, Rosière CA, Hagemann S, Zucchetti M, Baars FJ, Morais R, Andrade I (2008) Hydrothermal origin for the jaspilite-hosted, giant Serra Norte iron ore deposits in the Carajás mineral province, Para State, Brazil. Rev Econ Geol 15:255−290

Figueiredo e Silva RC, Hagemann SG, Lobato LM, Rosière CA, Banks DA, Davidson GJ, Vennemann TW, Hergt JM (2013) Hydrothermal fluid processes and evolution of the giant Serra Norte jaspilite-hosted iron ore deposits, Carajás Mineral Province, Brazil. Econ Geol 108:739–779

Freitas BT, Warren LV, Boggiani PC, De Almeida RP, Piacentini T (2011) Tectono-sedimentary evolution of the Neoproterozoic BIF-bearing Jacadigo Group, SW-Brazil. Sed Geol 238:48–70

Graf JL Jr, O'Connor EA, van Leeuwen P (1994) Rare earth element evidence of origin and depositional environment of Late Proterozoic ironstone beds and manganese-oxide deposits, SW Brazil and SE Bolivia. J S Am Earth Sci 7:115–133

Gutzmer J, Mukhopadhyay J, Beukes NJ, Pack A, Hayashi K, Sharp ZD (2006) Oxygen isotope composition of hematite and genesis of high-grade BIF-hosted iron ores. Geol Soc Am Mem 198:257–268

Hagemann SG, Barley ME, Folkert SL (1999) A hydrothermal origin for the giant BIF-hosted Tom Price iron ore deposit. In: Stanley CJ (ed) Mineral deposits, processes to processing. Balkema, Rotterdam, pp 41–44

Hagemann SG, Angerer T, Duuring P, Rosière CA, Figueiredo e Silva RC, Lobato L, Hensler AS, Walde D (2016) BIF-hosted iron mineral system: a review. Ore Geol Rev 76:317−359

Hagemann SG, Angerer T, Duuring P (2017) Iron ore systems in Western Australia. Austr Inst Mining Metall Mon 32:59–62

Hensler AS, Hagemann SG, Brown PE, Rosiere CA (2014) Using oxygen isotope chemistry to track hydrothermal processes and fluid sources in BIF-hosted iron ore deposits in the Quadrilátero Ferrífero, Minas Gerais, Brazil. Miner Deposita 49:293–311

Hensler AS, Hagemann SG, Rosière CA, Angerer T, Gilbert S (2015) Hydrothermal and metamorphic fluid-rock interaction associated with hypogene "hard" iron ore mineralisation in the Quadrilátero Ferrífero, Brazil: implications from in-situ laser ablation ICP-MS iron oxide chemistry. Ore Geol Rev 69:325–351

Hoefs J, Müller G, Schuster AK (1982) Polymetamorphic relations in iron ores from the Iron Quadrangle, Brazil: the correlation of oxygen isotope variations with deformation history. Contrib Miner Petrol 79:241–251

Hoefs J, Müller G, Schuster KA, Walde D (1987) The Fe-Mn ore deposits of Urucum, Brazil: an oxygen isotope study. Chem Geol 65:311–319

Klein C (2005) Some Precambrian banded iron-formations (BIFs) from around the world: their age, geologic setting, mineralogy, metamorphism, geochemistry, and origin. Am Miner 90:1473–1499

Klein C, Ladeira EA (2004) Geochemistry and mineralogy of Neoproterozoic banded iron-formations and some selected, siliceous manganese formations from the Urucum district, Mato Grosso do Sul, Brazil. Econ Geol 99:1233–1244

Knauth LP, Epstein S (1976) Hydrogen and oxygen isotope ratios in nodular and bedded cherts. Geochim Cosmochim Acta 40:1095–1108

Kyser TK, Kerrich R (1990) Geochemistry of fluids in tectonically active crustal regions. Mineral Assoc Can Short Course Ser 18:133–230

Land JS (2013) Genesis of BIF-hosted hematite iron ore deposits in the central part of the Maremane Anticline, Northern Cape Province, South Africa. Unpublished MSc thesis, Rhodes University, 112 p

Lindenmayer ZG, Fleck A, Gomes CH, Santos ABZ, Caron R, Paula FC, Laux JH, Pimentel MM, Sardinha AS (2005) Caracterização geológica do Alvo Estrela (Cu-Au), Serra dos Carajás, Pará. In: Marini OJ, Queiroz ET, and Ramos BW (eds) Caracterização de depósitos minerais em distritos mineiros da Amazônia. DNPM/CT-Mineral/FINEP/ADIMB, Brasília, pp 157−226

Lobato LM, Figueiredo e Silva RC, Hagemann S, Thorne W, Zucchetti M (2008) Hypogene alteration associated with high-grade BIF-related iron ore. Rev Econ Geol 15:107−128

Matsuhisa Y, Goldsmith JR, Clayton RN (1979) Oxygen isotopic fractionation in the system quartz-albite-anorthite-water. Geochim Cosmochim Acta 43:1131–1140

Matthews A, Goldsmith J, Clayton RN (1983) On the mechanisms and kinetics of oxygen isotope exchange in quartz and feldspars at elevated temperatures and pressures. Geol Soc Am Bull 94:396–412

Ministerio de Minas e Energia (2009) Quaresma LF, Produto 09—Minério de Ferro, Relatório Técnico 18, Perfil da Mineração de Ferro

Moore JM, Kuhn BK, Mark DF, Tsikos H (2011) A sugilite-bearing assemblage from the Wolhaarkop breccia, Bruce iron-ore mine, South Africa: evidence for alkali metasomatism and ^{40}Ar–^{39}Ar dating. Eur J Miner 23:661–673

Morgan R, Orberger B, Rosière CA, Wirth R, Carvalho CdM, Bellver-Baca MT (2013) The origin of coexisting carbonates in banded iron formations: a micromineralogical study of the 2.4 Ga Itabira Group, Brazil. Precambrian Res 224:491–511

Morris RC (1985) Genesis of iron ore in banded iron-formation by supergene and supergene-metamorphic processes—a conceptual model. In: Wolf KH (ed) Handbook of strata-bound and stratiform ore deposits. Elsevier, Amsterdam, pp 73–235

Morris RC, Kneeshaw M (2011) Genesis modelling for the Hamersley BIF-hosted iron ores of Western Australia: a critical review. Austr J Earth Sci 58:417–451

Netshiozwi ST (2002) Origin of high-grade hematite ores at Thabazimbi Mine, Limpopo Province, South Africa. Unpublished MSc thesis, Rand Afrikaans University, 135 p

Oliveira LARd, Rosière CA, Rios FJ, Andrade S, Moraes Rd (2015) Chemical fingerprint of iron oxides related to iron enrichment of banded iron formation from the Cauê Formation—Esperança Deposit, Quadrilátero Ferrífero, Brazil: a laser ablation ICP-MS study. Braz J Geol 45:193–216

Ohmoto H (1986) Stable isotope geochemistry of ore deposits. Rev Mineral 16:491–560

Papadopoulos V (2016) Mineralogical and geochemical constraints on the origin, alteration history and metallogenic significance of the Manganore iron-formation, Northern Cape Province, South Africa. Unpublished MSc thesis, Rhodes University, 201 p

Piacentini T, Vasconcelos PM, Farley KA (2013) $^{40}Ar/^{39}Ar$ constraints on the age and thermal history of the Urucum Neoproterozoic banded iron-formation, Brazil. Precambrian Res 228:48–62

Powell CM, Oliver NHS, Li Z-X, Martin DM, Ronaszeki J (1999) Synorogenic hydrothermal origin for giant Hamersley iron oxide ore bodies. Geology 27:175–178

Ribeiro A, Suita MTF, Sial AN, Fallick T, Ely F (2007) Geoquímica de isótopos estáveis (C, S, O) das rochas encaixantes e do minério de Cu(Au) do depósito Cristalino, Província Mineral de Carajás, Pará [abs.]: Congresso Brasileiro de Geoquímica, XI, Atibaia, Brazil vol 1, pp 1−4

Ridley JL (1997) Syn-metamorphic gold deposits in amphibolite and granulite facies rocks. Mitt Österr Miner Ges 142:101–110

Rosière CA, Baars FJ, Seoane JCS, Lobato LM, da Silva LL, de Souza SRC, Mendes GE (2006) Structure and iron mineralisation of the Carajás Province. Trans Inst Mining Metall Sect B 115:B126–B136

Rosière CA, Spier CA, Rios FJ, Suckau V (2008) The itabirites of the Quadrilátero Ferrífero and related high-grade iron ore deposits: an overview. Rev Econ Geol 15:223–254

Roy S, Venkatesh AS (2009) Mineralogy and geochemistry of banded iron formation and iron ores from eastern India with implications on their genesis. J Earth Sys Sci 118:619–641

Smith AJB, Beukes NJ (2016) Palaeoproterozoic banded iron formation-hosted high-grade hematite iron ore deposits of the Transvaal Supergroup, South Africa. Episodes 6:269–284

Spier CA, de Oliveira SMB, Sial AN, Rios FJ (2007) Geochemistry and genesis of the banded iron formations of the Caue Formation, Quadrilátero Ferrífero, Minas Gerais, Brazil. Precambrian Res 152:170–206

Spier CA, de Oliveira SMB, Rosiere CA, Ardisson JD (2008) Mineralogy and trace-element geochemistry of the high-grade iron ores of the Aguas Claras Mine and comparison with the Capao Xavier and Tamandua iron ore deposits, Quadrilátero Ferrifero, Brazil. Miner Deposita 43:229–254

Taylor HP Jr (1974) The application of hydrogen isotope problems of hydrothermal alteration and ore deposition. Econ Geol 69:843–883

Taylor D, Dalstra HJ, Harding AE, Broadbent GC, Barley ME (2001) Genesis of high-grade hematite orebodies of the Hamersley province, Western Australia. Econ Geol 96:837–873

Thorne WS, Hagemann SG, Barley M (2004) Petrographic and geochemical evidence for hydrothermal evolution of the North Deposit, Mt Tom Price, Western Australia. Miner Deposita 39:766–783

Thorne WS, Hagemann SG, Webb A, Clout J (2008) Banded iron formation-related iron ore deposits of the Hamersley Province, Western Australia. Rev Econ Geol 15:197–222

Thorne W, Hagemann S, Vennemann T, Oliver N (2009) Oxygen isotope compositions of iron oxides from high-grade BIF-hosted iron ore deposits of the central Hamersley Province, Western Australia: constraints on the evolution of hydrothermal fluids. Econ Geol 104:1019–1035

Thorne WS, Hagemann SG, Sepe D, Dalstra HJ, Banks DA (2014) Structural control, hydrothermal alteration zonation, and fluid chemistry of the concealed, high-grade 4EE iron orebody at the Paraburdoo 4E deposit, Hamersley Province, Western Australia. Econ Geol 109:1529–1562

Trompette R, de Alvarenga CJS, Walde D (1998) Geological evolution of the Neoproterozoic Corumbá graben system (Brazil): depositional context of the stratified Fe and Mn ores of the Jacadigo Group. J S Am Earth Sci 11:587–597

Urban H, Stribrny B, Lippolt HJ (1992) Iron and manganese deposits of the Urucum District, Mato Grosso do Sul, Brazil. Econ Geol 87:1375–1392

Van Deventer WF (2009) Textural and geochemical evidence for a supergene origin of the Paleoproterozoic high-grade BIF-hosted iron ores of the Maremane Dome, Northern Cape Province, South Africa. Unpublished MSc thesis, University of Johannesburg, 107 p

Viehmann S, Bau M, Bühn B, Dantas EL, Andrade FRD, Walde DHG (2016) Geochemical characterisation of Neoproterozoic marine habitats: evidence from trace elements and Nd isotopes in the Urucum iron and manganese formations, Brazil. Precambrian Res 282: 74–96

Walde DH, Hagemann SG (2007) The Neoproterozoic Urucum/mutun Fe and Mn deposits in W-Brazil/SE-

Bolivia: assessment of ore deposit models. Z Dtsch Ges Geowiss 158:45–55

Yapp CJ (1990) Oxygen isotopes in iron (III) oxides 1. Mineral-Water Fractionation Factors. Chem Geol 85:329–335

Zheng Y-F (1991) Calculation of oxygen isotope fractionation in metal oxides. Geochim Cosmochim Acta 55:2299–2307

Zheng Y-F (1995) Oxygen isotope fractionation in magnetites: structural effect and oxygen inheritance. Geochim Cosmochim Acta 121:309–316